[Chem. Pharm. Bull. 30(1) 7—16 (1982)]

Liquid-Solid Mass Transfer in Packed-Bed Reactors with Porous Particles[1)]

Yoshiharu Nishimura, Shushi Morita, and Jutaro Okada*

Faculty of Pharmaceutical Sciences, Kyoto University, Yoshida-Shimoadachi-cho Sakyo-ku, Kyoto, 606, Japan

(Received June 6, 1981)

Three different experiments were carried out in order to estimate the liquid-solid mass transfer coefficient (k_S) in a packed bed with porous particles. The experiments were, (A) liquid-phase hydrogenation of maleic acid on Pd–Al_2O_3, (B) hydrolysis of ethyl acetate on Amberlite 200C, and (C) moment analysis of in-pulse response curve in a packed bed of Amberlite XAD-2. Data were taken at low liquid feed rates and with small particles. The mass transfer factor (j_D) which is dimensionless with respect to k_S was correlated with the particle Reynolds number (Re_P). The obtained values of j_D were much lower than those expected from previous correlations obtained from the dissolution of nonporous particles. The results suggested that the effective mass transfer area (a_S) between liquid and porous particles was less than the geometrical outer surface area of the particles. a_S was considered to be influenced by the stagnant hold-up and the pore openings.

Keywords——liquid-solid mass transfer; packed-bed with porous particles; mass transfer factor; effective mass transfer area; hydrogenation of maleic acid; hydrolysis of ethyl acetate; moment analysis

Packed-bed reactors with porous catalyst particles are often used in the pharmaceutical industry. One of the factors which influence the global rate of reaction in the reactors is the mass transfer of the limiting reactant to the catalyst surface. Therefore, the mass transfer coefficient between the surface of the catalyst particle and the bulk liquid is important in reactor design. The mass transfer factor (j_D) which is dimensionless with respect to this coefficient is correlated with the particle Reynolds number (Re_P), and a number of correlations have been reported, but the agreement between them seems to be poor. In addition, most of them were determined by dissolution of nonporous particles (for example, benzoic acid or β-naphthol) into water,[2)] or by reaction with a nonporous solid.[3)] Since the catalyst particles which are used in a liquid-solid reaction system are porous, the above correlations are inadequate. Recently, in the hydrogenation of α-methylstyrene on porous Pd–Al_2O_3 catalyst, Morita *et al.* and Herskowitz *et al.* reported considerably lower values of j_D than those estimated from the correlations.[4,5)]

The purpose of this work was to estimate the liquid-solid mass transfer coefficient in a packed bed with porous particles by means of three different methods, and to compare the results with previous correlations. The three experiments were as follows;

Experiment A: Liquid-phase hydrogenation of maleic acid on a porous Pd-Al_2O_3 catalyst.

Experiment B: Liquid-phase hydrolysis of ethyl acetate on a porous macroreticular-type resin, Amberlite 200C.

Experiment C: Moment analysis of in-pulse response curve in a packed bed of porous polystyrene resin, Amberlite XAD-2.

Experimental

A. Liquid-Phase Hydrogenation of Maleic Acid on a Pd-Al_2O_3 Catalyst——0.5% Pd–Al_2O_3 particles were used as the catalyst. The preparation method was the same as that described in the previous paper.[6)] Particles with average sizes of 0.055 cm (28 to 32 mesh) and 0.110 cm (14 to 16 mesh) were chosen for the experiments. The physical properties of the catalyst are listed in Table I.

Fig. 1 shows a schematic diagram of the apparatus used. In a constant-temperature bath 1, an aqueous or ethanolic solution of maleic acid in a polyethylene feed reservoir 2 (20 l) was saturated with hydrogen by

TABLE I. Physical Properties of Particles

Experiment	A	B	C	
Particle	Al_2O_3	Amberlite 200C	Glass beads	Amberlite XAD-2
Pore volume, cm^3/g	0.53[a]	0.38[f]	0	0.65[c]
Solid phase density, ρ_S, g/cm^3	3.40[e]	1.468[b]	2.48[e]	1.081[c]
Particle density, ρ_P, g/cm^3	1.21[f]	0.944[b]	2.48[f]	0.656[f]
Bulk density, ρ_B, g/cm^3	0.72[e]	0.576[f]	1.56[e]	0.413[f]
Porosity of particles, ε_P	0.644[f]	0.357[b]	0	0.393[c]
Void fraction of bed, ε_B	0.405[f]	0.390[e]	0.371[f]	0.371[d]

a) From Sumitomo Chemical Ind., Ltd. *b*) N, Houjo, "Chelete Resins and Ion-Exchange Resins," Kodansha, 1976, p. 150. *c*) From Rohm and Haas Co. *d*) Assumed to be the same value as for glass beads. *e*) Measured. *f*) Calculated.

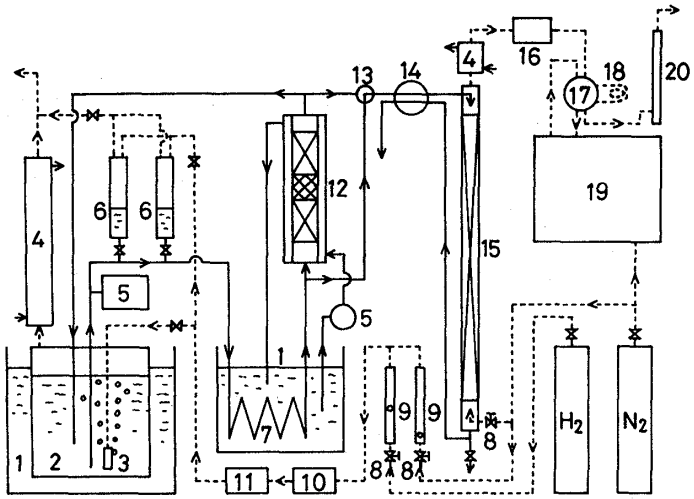

Fig. 1. Schematic Diagram of Apparatus used in Experiment A

1, constant temperature bath; 2, feed reservoir; 3, dispersion tube; 4, cooler; 5, pump; 6, surge tank; 7, preheater; 8, needle valve; 9, rotameter, 10, deoxygenator ($Pd-Al_2O_3$); 11, drier (silica gel); 12, liquid-full reactor; 13, three-way valve; 14, tube pump; 15, stripping column; 16, drier ($CaCl_2$); 17, six-way valve; 18, gas sampler; 19, gas chromatograph; 20, soap film meter; ----→----, gas flow line; ——→——, liquid flow line.

continuous bubbling. Hydrogen supplied to the feed reservoir was purified by passing it through beds of $Pd-Al_2O_3$ followed by silica gel. The solution was introduced into the reactor 12 by the pump 5. To avoid pulse flow, two surge tanks 6 were introduced into the feed line.

The glass reactor was 1.08 cm i.d. and the temperature was kept constant by circulation of water from the constant-temperature bath through the jacket. The catalyst particles were supported by a 100 mesh stainless steel screen. After passing through the reactor, the effluent was recycled to the reservoir.

The liquid feed rate was adjusted in such a way that the conversion of dissolved hydrogen per pass through the reactor was less than 30%. Thus, the operation was regarded as a differential one. The concentration of maleic acid in the reactor was several hundred times higher than that of hydrogen in the liquid, so that it was essentially uniform during a run. Ethanol or water was used as the solvent. Table II shows the experimental conditions.

The solutions at the inlet and outlet of the reactor were alternately introduced into the stripping column 15 at a constant flow rate by the pump 14. The column was a 2.5 cm i.d. and 150 cm long glass column packed with 2—4 mm glass beads. Here, nitrogen was used to remove the dissolved hydrogen from the liquid. The amount of hydrogen in the mixed gas was measured with a gas chromatograph 19. Then, the conversion of hydrogen per pass, x [—], was calculated. For the differential reactor in the steady state, the global rate of reaction, R_S [mol/(g of catalyst)(s)], was calculated as follows

$$R_S = \frac{Q_L C_I x}{m} \tag{1}$$

where Q_L [cm^3/s] is the volumetric liquid feed rate, C_I [mol/cm^3] is the concentration of hydrogen in the liquid entering the reactor, and m [g] is the mass of catalyst in the reactor.

Table II. Experimental Conditions

A. Liquid-phase hydrogenation of maleic acid on $Pd-Al_2O_3$	
Palladium content, wt%	0.5
Catalyst particle size, d_P, cm	0.110[a], 0.055[b]
Solvent	EtOH, H_2O
Mass of catalyst in reactor, m, g	2.0, 1.0(EtOH); 1.0, 0.5 (H_2O)
Concentration of H_2 at inlet of reactor, C_I, mol/cm^3	3.58×10^{-6} (EtOH); 7.32×10^{-7} (H_2O)
Initial concentration of maleic acid, mol/cm^3	0.5×10^{-3} (EtOH); 0.2×10^{-3} (H_2O)
Pressure of H_2 in absorber, atm	1.0
Temperature of absorber, °C	30 (EtOH); 40 (H_2O)
Liquid feed rate, Q_L, cm^3/s	0.60—3.61
Reaction temperature, °C	40, 30, 22 (EtOH); 40, 30 (H_2O)
B. Hydrolysis of ethyl acetate on Amberlite 200C	
Catalyst particle size, d_P, cm	0.110[a], 0.055[b]
Mass of catalyst in reactor, m, g	0.253 (d_P=0.110); 0.631, 0.243 (d_P=0.055)
Concentration of ethyl acetate at inlet of reactor, C_I, mol/cm^3	0.205×10^{-3}
Liquid feed rate, Q_L, cm^3/s	0.19×10^{-2}—3.84×10^{-2} (d_P=0.110); 0.31×10^{-2}—8.78×10^{-2} (d_P=0.055)
Reaction temperature, °C	61
C. Moment analysis of in-pulse response curve on Amberlite XAD-2	
Particle size, d_P, cm	0.075[b], 0.055[c], 0.043[d]
Liquid feed rate, Q_L, cm^3/s	1.33×10^{-2}—9.0×10^{-2}
Temperature, °C	30

a) 14 to 16 mesh. *b*) 20 to 24 mesh. *c*) 28 to 32 mesh. *d*) 32 to 42 mesh.

B. Hydrolysis of Ethyl Acetate on Amberlite 200C——The catalyst used was an ion-exchange resin of the strong acid type, Amberlite 200C (Rohm and Haas Company, U.S.A.), which had a porous structure (macroreticular type). The physical properties of the particles are given in Table I. After sieving the resin in distilled water, particles with average sizes of 0.055 cm and 0.110 cm were chosen for the reaction studies. In the glass reactor (0.98 cm i.d. and 20 cm long), Na^+-type resin was first converted into H^+-type by treating it with a large excess of aqueous HCl, followed by washing with distilled water till Cl^- ion was not detectable in the effluent.

The reaction was carried out by the flowing method; 0.205 M aqueous ethyl acetate was introduced at the top of the reactor. Since the feed solution was gradually hydrolyzed in the reservoir (though the conversion was less than 1% in a run), the concentration of acetic acid in the feed solution was measured before the solution entered the reactor. The experimental conditions are shown in Table II.

The conversion of ethyl acetate was kept below 30%, to ensure differential operation. Since there was no side reaction under the experimental conditions used, the amount of acetic acid produced was titrated with aqueous NaOH using phenolphthalein as an indicator. Then, the concentration of ethyl acetate in the effluent was calculated. The global rate of reaction was calculated by means of equation (1). In this case, C_I and x are the concentration of ethyl acetate in the liquid entering the reactor and the conversion of ethyl acetate, respectively.

C. Moment Analysis on In-Pulse Response Curve in Packed Bed of Amberlite XAD-2——The particles used were porous resin, *i.e.*, Amberlite XAD-2 (Rohm and Haas Company), and nonporous glass beads. To remove the impurities in the resin, the purchased XAD-2 was pretreated by the method of Relles *et al.*[7] Particles with average sizes of 0.043 cm (32 to 42 mesh), 0.055 cm (28 to 32 mesh) and 0.075 cm (20 to 24 mesh) were chosen, and packed into the column by means of tapping. The column was 1.02 cm i.d. and about 31 cm long. Distilled water was used as the mobile phase. The physical properties of the particles and the experimental conditions are shown in Table I and Table II, respectively.

Hexamminecobalt chloride was chosen as a tracer. About 30 μl of the saturated aqueous solution was instantaneously injected at the entrance of the column, and the time course of emergence of the tracer in the effluent was measured at 254 nm by means of a ultraviolet (UV) detector with a continuous flow cell. The absorbance was converted into concentration according to a predetermined calibration curve. It was confirmed in advance that the tracer was not adsorbed by XAD-2.

The first absolute moment, μ_1 [s], and the second central moment, μ'_2 [s^2], of the chromatographic peak can be calculated as follows

$$\mu_1 = \frac{\int_0^\infty Ctdt}{\int_0^\infty Cdt} \qquad (2)$$

$$\mu_2' = \frac{\int_0^\infty C(t-\mu_1)^2 dt}{\int_0^\infty C dt} \quad (3)$$

where t [s] is the time after the injection of the tracer, and C [mol/cm^3] is the concentration of the tracer in the effluent. The integrals were evaluated numerically from the experimental chromatographic peak using Simpson's rule. The limits (the start (t_s) and the end (t_e) of the peak) were taken as the times corresponding to peak height equal to 0.5% of the maximum, and the elution time ($=t_e-t_s$) was divided into more than 100 equal intervals.

Results and Data Analysis

A. Liquid-Phase Hydrogenation of Maleic Acid on a Pd-Al_2O_3 Catalyst

First, the absorption of hydrogen was measured by using 0.5% Pd-Al_2O_3 slurry catalyst in a batch reactor at 40°C and atmospheric pressure. One equivalent of hydrogen was absorbed, and succinic acid was formed in nearly 100% yield. Next, the time course of the catalyst activity was measured by using 0.5% Pd-Al_2O_3 particles in the packed bed reactor. The result indicated that the catalyst had a steady activity after it had been used for about 24 h. In subsequent experiments the data were taken in the constant activity period.

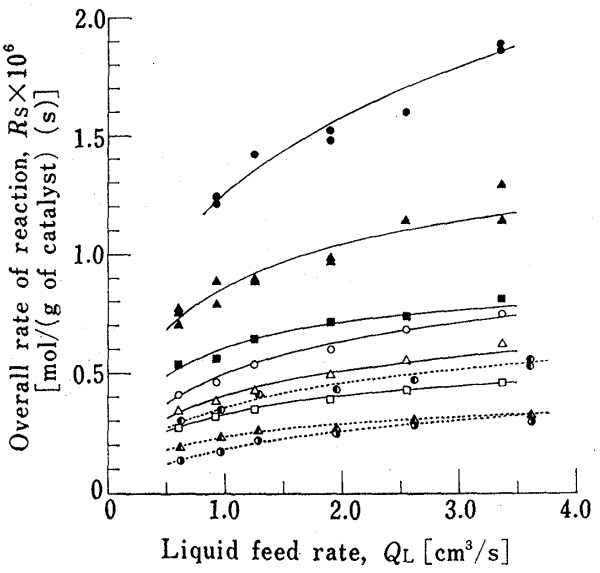

Fig. 2. Effect of Liquid Feed Rate on the Overall Rate of Reaction for Hydrogenation of Maleic Acid

Solvent, d_P(cm), temperature(°C): —□—, EtOH, 0.110, 22; —△—, EtOH, 0.110, 30; —○—, EtOH, 0.110, 40; —■— EtOH, 0.055, 22; —▲—, EtOH, 0.055, 30; —●— EtOH, 0.055, 40; ···◑···, H_2O, 0.110, 40; ···▲···, H_2O, 0.055, 30; ···◐··· H_2O, 0.055, 40.

Fig. 2 shows plots of R_S *vs.* Q_L. Increase in R_S with increasing Q_L suggests a significant effect of liquid-solid mass transfer. The solubility of hydrogen in liquid is very low (for example, the solubility of hydrogen in ethanol is 3.58×10^{-6} mol/cm^3 at 30°C[8]), so that the limiting reactant is hydrogen.

Kinetic studies concerning C=C double bond hydrogenation over Pd-Al_2O_3 suggest that the rate of chemical reaction is first order with respect to hydrogen concentration and zero order with respect to maleic acid concentration.[9]

At the steady state, the global rate of reaction can be expressed in terms of the mass transfer rate of the limiting reactant to the catalyst particles;

$$R_S = k\eta C_S = k_S a_S (C_B - C_S) \quad (4)$$

where k [cm^3/(g of catalyst)(s)] is the intrinsic, first-order rate constant, η [—] is the effectiveness factor, C_S [mol/cm^3] is the hydrogen concentration in the liquid at the surface of the catalyst particle, k_S [cm/s] is the liquid-solid mass transfer coefficient, and a_S [cm^2/(g of catalyst)] is the effective liquid-solid mass transfer area per unit mass of catalyst. The average hydrogen concentration in the bulk liquid, C_B [mol/cm^3], can be written as

$$C_B = C_I(1-x/2) \quad (5)$$

Eliminating C_S from equation (4),

$$\frac{C_B}{R_S} = \frac{1}{k\eta} + \frac{1}{k_S a_S} \quad (6)$$

The mass transfer factor, j_D [—], can be conveniently correlated to the powder function of the particle Reynolds number, Re_P [—], based on the particle diameter, d_P [cm].

$$j_D = \frac{k_S}{u_L} Sc^{2/3} = \beta Re_P^{-\alpha} \tag{7}$$

$$Sc = \frac{\mu_L}{D\rho_L} \tag{8}$$

$$Re_P = \frac{d_P u_L \rho_L}{\mu_L} \tag{9}$$

where α and β are the parameters, u_L [cm/s] is the superficial velocity of the liquid, Sc [—] is the Schmidt number, D [cm^2/s] is the molecular diffusivity of oxygen in the liquid, and ρ_L [g/cm^3] and μ_L [g/(cm·s)] are the density and viscosity of the liquid, respectively.

The liquid-solid mass transfer area can be calculated by supposing that the particles are spherical, so that

$$a_S = \frac{6}{d_P \rho_P} \tag{10}$$

where ρ_P [g/cm^3] is the particle density. Substituting equations (7) to (10) into equation (6),

$$\frac{C_B}{R_S} = \frac{1}{k\eta} + \frac{1}{\beta} X \tag{11}$$

where

$$X = \frac{d_P^2 \rho_P \rho_L}{6\mu_L} Sc^{2/3} \cdot Re_P^{\alpha-1} \tag{12}$$

Equation (11) means that (C_B/R_S) should be related by a straight line with an intercept of $(1/k\eta)$ and a slope of $(1/\beta)$ to a variable X. Therefore, when a line is estimated from a set of data taken by changing the liquid feed rate for a given particle size, reaction temperature and solvent, the lines obtained should be parallel to each other. Note that η is independent of C_S because of the first-order, irreversible reaction.

Parameters α and β may be estimated as follows. Assigning a value of α, the slope for each set of data can be calculated by the least-squares method. The optimum value of α may be estimated when the coefficient of variation for $(1/\beta)$ is minimum.

The molecular diffusivity of hydrogen in the reaction mixture was assumed to be identical with that in water or ethanol.[10] At α=0.36, the coefficient of variation for $(1/\beta)$ was found to be minimum and the mean of $(1/\beta)$ was 1.506; thus, the following correlation for j_D was obtained.

$$j_D = 0.664\, Re_P^{-0.36} \qquad (2.5 < Re_P < 65) \tag{13}$$

Fig. 3 shows the linear plots at α=0.36. Under the experimental conditions used, the slopes are nearly parallel to each other.

B. Hydrolysis of Ethyl Acetate on Amberlite 200C

Since a large excess of water compared to ethyl acetate (about 270-fold molar excess) was used and the conversion of ethyl acetate was low, this reaction was essentially irreversible. From kinetic studies,[11] the rate of reaction is first order with respect to the concentration of ethyl acetate. Therefore, equations (4) to (9) are obtainable by replacing the nomenclatures for hydrogen with those for ethyl acetate.

$$\frac{R_S}{C_B} = \frac{1}{\dfrac{1}{k\eta} + \dfrac{1}{k_S a_S}} \tag{14}$$

Fig. 4 shows plots of (R_S/C_B) against Q_L based on equation (4). In the range of low Q_L, (R_S/C_B) is largely dependent on Q_L, indicating that the liquid-solid mass transfer resistance, $(1/k_S a_S)$,

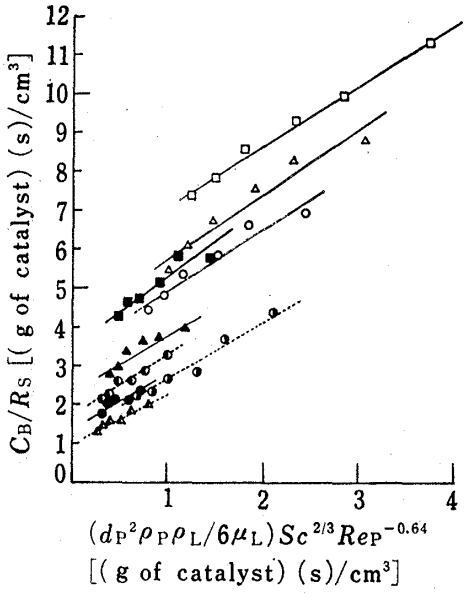

Fig. 3. Plots at $\alpha=0.36$ for Hydrogenation of Maleic Acid

Symbols: as in Fig. 2.

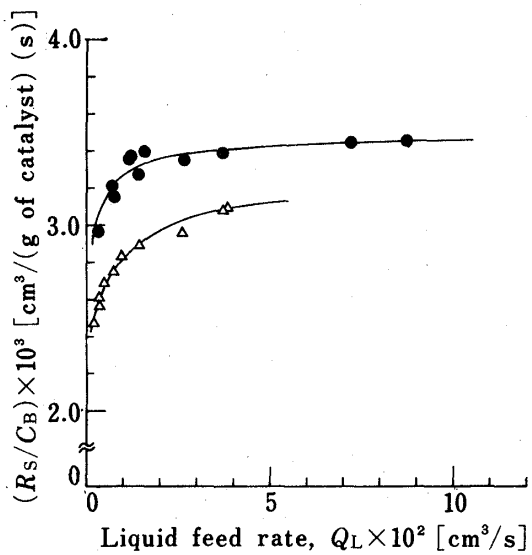

Fig. 4. Effect of Liquid Feed Rate on (R_S/C_B) for Hydrolysis of Ethyl Acetate

●, 28—32 mesh; △, 14 to 16 mesh.

is significant. As Q_L increases, (R_S/C_B) approaches a constant value, indicating that the resistance is insignificant. When Q_L approaches infinity, $(1/k_Sa_S)$ approaches zero, so that $k\eta=\lim_{Q_L\to\infty}(R_S/C_B)$.

To estimate $k\eta$ from Fig. 4, the regression equation was postulated to be hyperbolic:

$$\frac{R_S}{C_B} = b_0 + \frac{b_2}{Q_L-b_1} \tag{15}$$

where b_0, b_1 and b_2 are the parameters and $b_0=k\eta$. The values of $k\eta$ estimated by the nonlinear least-squares method were 3.51×10^{-3} and 3.24×10^{-3} [cm^3/(g of catalyst) (s)] for $d_P=0.055$ cm and $d_P=0.110$ cm, respectively. Using these values, k_Sa_S was calculated from equation (6). Next, k_S was isolated by the use of equation (10), and j_D was correlated with Re_P by the least-squares method as follows;

$$j_D = 0.727\,Re_P^{-0.34} \tag{16}$$

C. Moment Analysis of In-Pulse Response Curve in a Packed Bed of Amberlite XAD-2

The tracer used is not adsorbed by XAD-2, as mentioned in the experimental section, so that the mass balance equations in the fixed bed and in the particles can be expressed by the equations (17) and (18), respectively.

$$\frac{\partial C}{\partial t} = \frac{D_L}{\varepsilon_B}\frac{\partial^2 C}{\partial z^2} - u\frac{\partial C}{\partial z} - \frac{3D_e}{r_S}\left(\frac{1-\varepsilon_B}{\varepsilon_B}\right)\left(\frac{\partial C_i}{\partial r}\right)_{r=r_S} \tag{17}$$

$$\frac{\partial C_i}{\partial t} = \frac{D_e}{\varepsilon_P}\left(\frac{\partial^2 C_i}{\partial r^2}+\frac{2}{r}\frac{\partial C_i}{\partial r}\right) \tag{18}$$

with the following boundary and initial conditions;

$$D_e\left(\frac{\partial C_i}{\partial r}\right)_{r=r_S} = k_S\{C-(C_i)_{r=r_S}\} \tag{19}$$

$$\frac{\partial C_i}{\partial r} = 0 \qquad \text{at } r = 0 \tag{20}$$

$$\left.\begin{aligned} C &= 0 && \text{at } t = 0\\ C_i &= 0 && \text{at } t = 0\\ C &= \delta && \text{at } z = 0,\ t = 0 \end{aligned}\right\} \tag{21}$$

where C [mol/cm^3] and C_i [mol/cm^3] are the tracer concentrations in the bulk liquid and in the pores, t [s] is the time, D_L [cm^2/s] and D_e [cm^2/s] are the axial dispersion coefficient and the effective diffusivity in the pores, r [cm] and r_S [cm] are the radial distance in the particle and the particle radius, z [cm] is the axial distance in the bed, ε_B [—] and ε_P [—] are the interparticle and intraparticle void fractions, and δ is the Dirac delta function, which has an infinite value at $t=0$.

Equations (17) and (18) with equations (19) to (21) were solved in the Laplace domain by Schneider *et al.*,[12] and the first absolute moment of the response curve, μ_1 [s], and the second central moment, μ_2' [s^2], were given by

$$\mu_1 = \frac{L}{u}\left\{1+\frac{1-\varepsilon_B}{\varepsilon_B}\varepsilon_P\right\} \tag{22}$$

$$\mu_2' = \frac{2L}{u}\left[\frac{1-\varepsilon_B}{\varepsilon_B}\varepsilon_P\left\{\frac{r_S^2\varepsilon_P}{15}\left(\frac{1}{D_e}+\frac{5}{k_S r_S}\right)\right\} + \frac{D_L}{u^2\varepsilon_B}\left(1+\frac{1-\varepsilon_B}{\varepsilon_B}\varepsilon_P\right)^2\right] \tag{23}$$

where u [cm/s] is the interstitial velocity in the bed and L [cm] is the length of the bed.

First, μ_1 and μ_2' were measured by using a column packed with nonporous glass beads in order to estimate the axial dispersion coefficient in the bed. In the case of glass beads $\varepsilon_P=0$, so that equations (22) and (23) can be simplified to

$$\mu_1 = \frac{L}{u} \tag{24}$$

$$\mu_2' = \frac{2L}{\varepsilon_B u^3} D_L \tag{25}$$

Fig. 5 shows the plots of μ_1 *vs.* $(1/u)$. Regardless of the particle size, a linear relationship existed, which could be expressed as

$$\mu_1 = 31.18(1/u) + 6.11 \tag{26}$$

On comparing equation (24) with equation (26), $L=31.18$ [cm] was obtained, in agreement with the height of the packed bed used. The intercept shows that the dead time was about 6 s. This dead time was so short compared to the average residence time that it was not considered in data analysis for the subsequent experiments. Fig. 6 shows plots of the Peclet number, Pe [—] $(=u_L d_P/D_L)$, against the modified particle Reynolds number, Re_P' [—] $(=u_L d_P \rho_L/\{(1-\varepsilon_B)\mu_L\})$. The linear relationship could be expressed as

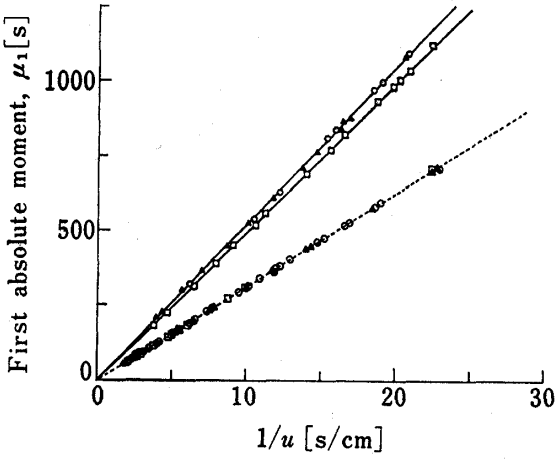

Fig. 5. First Absolute Moment *vs.* Reciprocal of the Interstitial Velocity

□, 20—24 mesh; ○, 28—32 mesh; ▲, 32—42 mesh; ——, Amberlite XAD-2; ----, glass beads.

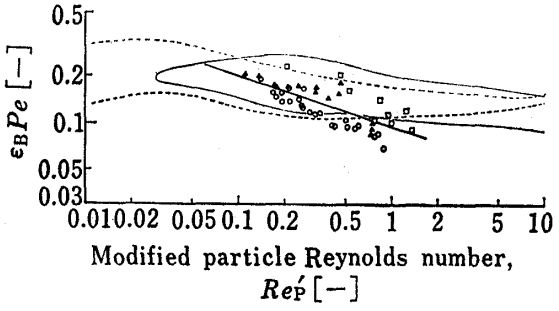

Fig. 6. Relation between Peclet Number and Modified Particle Reynolds Number

Symbols: as in Fig. 5.
⬭, Ebach and White; ⬭, Miller and King.

$$\varepsilon_B Pe = 0.095(Re_P')^{-0.323} \tag{27}$$

The ranges surrounded by the solid and dotted curves in Fig. 6 show the results of Ebach *et al.* and Miller *et al.*[13] As our data accord well with theirs, equation (27) was used in data analysis.

Next, μ_1 and μ_2' were measured by using the column packed with porous particles, XAD-2. Fig. 5 shows the plots of μ_1 *vs.* $(1/u)$. A little difference exists between the particles of different size, but each gives a good linear relationship. The difference of μ_1 from that of glass beads for the same value of $(1/u)$ shows the extension of the average residence time. For the particles of 20—24 mesh (d_P=0.075 cm), 28—32 mesh (d_P=0.055 cm) and 32—42 mesh (d_P=0.043 cm), the values of ε_P=0.390, 0.391 and 0.340 were obtained from equation (22), respectively. ε_P for d_P=0.043 cm was somewhat different from the others, but the values obtained accorded approximately with the published value for XAD-2 (ε_P=0.393 by the mercury penetration method). The obtained ε_P for each particle size was used in data analysis.

Combining equation (22) with equation (23) gives

$$Y = \frac{1}{D_e} + \frac{5}{k_S r_S} = \frac{\dfrac{\mu_2'}{\mu_1} - \dfrac{D_L}{u^2\varepsilon_B}\left(1+\dfrac{1-\varepsilon_B}{\varepsilon_B}\varepsilon_P\right)}{\dfrac{2(1-\varepsilon_B)\varepsilon_P^2 r_S^2}{15\{\varepsilon_B+(1-\varepsilon_B)\varepsilon_P\}}} \tag{28}$$

The use of equation (7) for k_S yields

$$Y = \frac{1}{D_e} + \frac{10\rho_L}{\beta\mu_L} Sc^{2/3} \cdot Re_P^{\alpha-1} \tag{29}$$

Equation (29) shows that, if α is known, plots of the right-hand term of equation (28), which can be obtained from the measured moments, against $Re_P^{\alpha-1}$ give a straight line with an intercept of $(1/D_e)$ and a slope of $(10\rho_L Sc^{2/3}/(\beta\mu_L))$ irrespective of the particle size. Assigning a value to α, the coefficient of correlation between Y and $Re_P^{\alpha-1}$ was calculated. At α=0.32 the coefficient was maximum. Fig. 7 shows the linear plots at α=0.32. The regression equation is

$$\frac{1}{D_e} + \frac{5}{k_S r_S} = (0.814 + 0.179\, Re_P^{-0.68}) \times 10^6 \tag{30}$$

From the slope, α=0.32 was obtained. The molecular diffusivity of the tracer in water, D, contained in Sc, was estimated ($D=1.56\times10^{-5}$ cm^2/s at 30°C) from the Nernst–Haskell

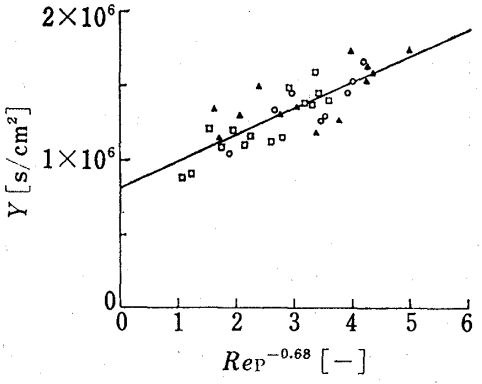

Fig. 7. Y *vs.* $Re_P^{\alpha-1}$ at α=0.32

Symbols: as in Fig. 5.

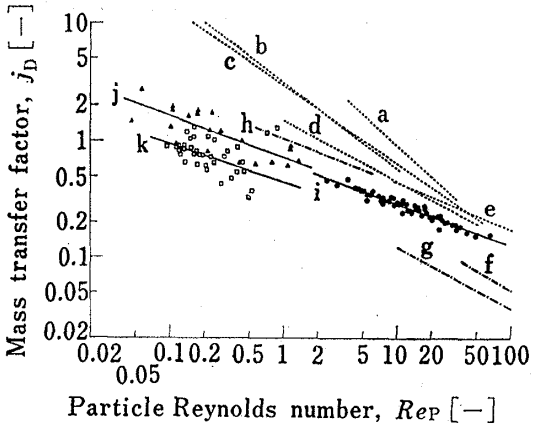

Fig. 8. Mass Transfer Factor *vs.* Particle Reynolds Number

●, experiment A; ▲, experiment B; □, experiment C. a, Hobson *et al.*; b, Dwivedi *et al.* (ε_B=0.37); c, Wilson *et al.* (ε_B=0.37); d, Evans *et al.*; e, Sherwood *et al.*; f, Morita *et al.* (d_P=0.141 cm); g, Morita *et al.* (d_P=0.0541 cm); h, Ali Kahn *et al.*; i, equation (13); j, equation (16); k, equation (31).

equation.[14] The intercept of the line gives $D_e=1.23\times10^{-6}$ [cm^2/s]. Thus, the tortuosity factor, τ [—] ($=D\varepsilon_P/D_e$), is 4.7. Tortuosity factors of the order of 2 to 6 have been reported in a number of investigations of many kinds of porous particles,[4,6,9b,15] so that the obtained value of D_e is reasonable. The estimated values of α and β give the following correlation for j_D;

$$j_D = 0.45\,Re_P^{-0.32} \tag{31}$$

Discussion

Three correlations for j_D, obtained from experiments A, B and C, are shown in Fig. 8. Though the correlations were obtained by three different methods, they were similar.

The dotted straight lines are some reported correlations obtained from the dissolution of nonporous particles. The correlations of Dwivedi *et al.*[16] and Sherwood *et al.*[17] are reanalyzed ones based on a number of previous experimental data. The chained straight lines are the results of Morita *et al.*, which were obtained from the hydrogenation of α-methylstyrene on porous Pd–Al_2O_3 catalyst.[4] The correlation of Ali Khan *et al.*[6] is also shown in Fig. 8, and was estimated from the liquid-phase oxidation of diethanolamine on porous Pd–Al_2O_3. The values of j_D obtained from our experiments and those of Ali Khan *et al.* and Morita *et al.* are much lower than the previous correlations based on the dissolution experiments.

The main reason for the difference in j_D between the dissolution experiments and the reaction or tracer experiments is considered to be differences in the effective liquid-solid surface area for mass transfer. In particular, we consider that the stagnant liquid zone at the particle contact points greatly influences the effective surface area. In the dissolution system, the liquid in this zone may be nearly saturated with the dissolved substance and elution is carried out at the interface between the flowing liquid and the stagnant liquid, so that the particle surface in this zone is considered to be almost wholly effective for mass transfer. On the other hand, in the reaction or tracer system, the reactant or tracer must be transferred to the particle surface. Because of the low diffusivity in the liquid, the rate of mass transfer from the interface to the particle surface in the stagnant zone is very slow, so that the surface is considered not to be effective for mass transfer. But, when the reaction is slow, this zone is moderately effective. When the reaction is very slow and the surface reaction is the rate-determining step, the influence of stagnant liquid is insignificant. A similar explanation has been suggested for the contacting efficiency in trickle-bed reactors.[18] In the case of the pulse response method, the tracer diffused from the flowing liquid to the stagnant liquid must return again to the flowing liquid in a short time. Therefore, the particle surface in contact with the stagnant liquid may not contribute appreciably to the liquid-solid mass transfer. Supposing that the particle surface in contact with the stagnant liquid is not effective for mass transfer in the reaction or pulse response system, the effective surface area was calculated roughly. The stagnant hold-up, h_S [—] (defined as the fracton of the volume occupied by stagnant liquid in the bed), was estimated as 0.05—0.1,[19] and the number of contact points as 6—9.[20] The results indicated that the effective area was 45—70% of that in the dissolution system, in which the effective surface area was assumed to be equal to the geometrical surface area calculated by equation (10).

Another reason for the difference in the effectve surface area may depend upon whether the particles are porous or nonporous. When the particles are porous, the average diameter of the pore openings and the fraction of the pore mouth area against the total external surface area may be significant factors. In the case of porous particles, the mass transfer is considered to be constrained to a region close to the pore openings on the outer surface of the particle, so that the effective surface area for mass transfer could be less. In a study of the hydrogenation of α-methylstyrene on porous Pd–Al_2O_3 catalyst, Herskowitz *et al.*[5] reported that their j_D agreed reasonably well with the j_D of Dwivedi *et al.*[16] when the effective surface area was

assumed to be the product of the total external surface area and the intraparticle void fraction.

In our data analysis, the effective surface area was assumed to be the geometrical surface area despite the large difference that must exist, so that the j_D obtained would be much lower than that of the correlations based on the dissolution experiments.

To sum up, the liquid-solid mass transfer rate in a packed bed of porous particles should be formulated in terms of the effective surface area, which depends mainly on the stagnant hold-up and pore openings. More studies will be needed on the factors which influence these properties, especially for samll particles and low liquid feed rates.

Acknowledgement We thank Y. Shirakura and C. Tabuchi for their assistance in the experimental work.

References and Notes

1) Parts of this work were presented at the 99th Annual Meeting of the Pharmaceutical Society of Japan, Sapporo-shi, Aug. 1980 and the 30th Annual Meeting of the Kinki Branch of the Pharmaceutical Society of Japan, Matsubara-shi, Nov. 1980.
2) G.C. Evans and C.F. Gerald, *Chem. Eng. Progr.*, **49**, 135 (1953); M. Hobson and G. Thodos, *ibid.*, **45**, 517 (1949); E.J. Wilson and C.J. Geankoplis, *Ind. Eng. Chem. Fundamentals*, **5**, 9 (1966).
3) T. Hirose, T. Mori, and Y. Sato, *J. Chem. Eng. Japan*, **9**, 220 (1976).
4) S. Morita and J.M. Smith, *Ind. Eng. Chem. Fundamentals*, **17**, 113 (1978).
5) M. Herskowitz, R.G. Carbonell, and J.M. Smith, *A.I. Ch. E. Journal*, **25**, 272 (1979).
6) M.I. Ali Khan, Y. Miwa, S. Morita, and J. Okada, *Chem. Pharm. Bull.*, **29**, 1802 (1981).
7) H.M. Relles and R.W. Schluenz, *J. Am. Chem. Soc.*, **96**, 6469 (1974).
8) Chemical Society of Japan (ed.), "Kagaku Benran (Kisohen)," Maruzen, Tokyo, 1966, p. 625.
9) *a*) B.O. Babcock, G.T. Mejdell, and O.A. Hougen, *A.I. Ch. E. Journal*, **3**, 366 (1957); *b*) C.N. Satterfield, Y.A. Ma, and T.K. Sherwood, *Int. Chem. Eng. Symp. Ser.*, **28**, 22 (1968).
10) Kagaku Kogaku Association (ed.), "Kagaku Kogaku Benran," 4th ed., Maruzen, Tokyo, 1978, p. 71.
11) K. Saito, *Kogyo Kagaku Zasshi*, **64**, 1738 (1961).
12) P. Schneider and J.M. Smith, *A.I. Ch. E. Journal*, **14**, 762 (1968).
13) E.A. Ebach and R.R. White, *A.I. Ch. E. Journal*, **4**, 161 (1958); S.F. Miller and C.J. King, *ibid.*, **12**, 767 (1966).
14) T.K. Sherwood, R.L. Pigford, and C.K. Wilke, "Mass Transfer," McGraw-Hill, New York, 1975, p. 35.
15) S.-H. Hsu and J.A. Ruether, *Ind. Eng. Chem. Process Des. Dev.*, **17**, 524 (1978); C.N. Satterfield, "Mass Transfer in Heterogeneous Catalysis," M.I.T. Press, Cambridge, Mass., 1970, p. 66, 157.
16) P.N. Dwivedi and S.N. Upadhyay, *Ind. Eng. Chem. Process Des. Dev.*, **16**, 157 (1977).
17) T.K. Sherwood, R.L. Pigford, and C.R. Wilke, "Mass Transfer," McGraw-Hill, New York, 1975, p. 242.
18) S. Sicardi, G. Baldi, A. Gianetto, and V. Specchia, *Chem. Eng. Sci.*, **35**, 67 (1980); S. Sicardi, G. Baldi, and V. Specchia, *ibid.*, **35**, 1775 (1980).
19) S. Goto and J.M. Smith, *A.I. Ch. E. Journal*, **21**, 706 (1975).
20) T. Kubo, G. Jinbo, E. Suito, H. Takahashi, and S. Hayakawa, (eds.), "Funtai," 2nd ed., Maruzen, Tokyo, 1979, p. 340.